THE ASTROPHYSICAL JOURNAL, 386:L23–L26, 1992 February 10

POSITIONS OF THE RADIO RECOMBINATION LINE MASERS IN MWC 349

P. PLANESAS AND J. MARTÍN-PINTADO
Centro Astronómico de Yebes (IGN), Apartado 148, E-19080 Guadalajara, Spain
AND
E. SERABYN
Department of Physics 320-47, California Institute of Technology, Pasadena, CA 91125
Received 1991 October 9; accepted 1991 November 21

ABSTRACT

The Owens Valley Millimeter Interferometer has been used at 232 GHz to measure the relative positions of the strongest H30α maser features toward MWC 349. Maser emission appears to originate from two positions 0".065 ± 0".005 (80 AU) apart, located in an almost east-west direction (P.A. 107° ± 7°), approximately perpendicular to the bipolar ionized wind structure observed in low-frequency radio continuum maps. We argue that the maser features originate in two positions associated with a nearly edge-on, neutral disk which is the source of high-density ionized gas. The maser spots probably arise from clumps located in the near part of the disk surface.

Subject headings: masers — radio lines: atomic — stars: individual (MWC 349) — stars: mass-loss — techniques: interferometric

1. INTRODUCTION

Strong radio recombination line maser emission has been detected for the first time toward the ionized wind region surrounding the star MWC 349 (Martín-Pintado et al. 1989a). The spectra of the H29α, H30α, and H31α lines show double-peaked profiles, with LSR velocities of −16 and +32 km s^{-1}. Maser emission has been found in the hydrogen alpha transitions observed toward this source at wavelengths between 1 and 2 mm (Martín-Pintado et al. 1989a), while at longer wavelengths the lines are much weaker and the profiles are approximately Gaussian. Subsequently, intensity variations on a time scale of a few months were observed (Martín-Pintado, Thum, & Bachiller 1989b), with one of the components increasing in intensity by almost a factor of 3 in a time span of 6 months, while the other one decreased by 20% in the same period of time. MWC 349 remains the only object where radio recombination maser lines have been detected to date; it is also the only example of radio recombination line variability.

MWC 349 has the radio continuum spectrum of an isothermal ionized stellar wind with constant expansion velocity (see, e.g., Olnon 1975), its spectrum being optically thick up to frequencies of 3000 GHz (100 μm). The evolutionary stage of this object is, however, unknown. Suggestions about its nature range from a young stellar object (Hamann & Simon 1986) to a post–main-sequence object (Thompson et al. 1977; Harvey, Thronson, & Gatley 1979). Some of the hypothesized objects imply some kind of asymmetry, consistent with some observations. In fact, high angular resolution VLA observations of the radio continuum emission of MWC 349 at 15 GHz show that the ionized gas is distributed in a 0".4 diameter region (~500 AU, assuming a distance of 1.2 kpc for MWC 349) with a bipolar structure that suggests the existence of an anisotropic wind (White & Becker 1985). However, nothing is known about the inclination to the line of sight and the radial velocity of the gas in the two continuum "lobes." Moreover, as suggested by near-IR spectroscopic observations (Hamann & Simon 1986, 1988), the kinematics of the gas within 3 AU of the star is more consistent with rotation than expansion. These authors suggested the existence of a rotating disk in a plane perpendicular to the bipolar ionized outflow.

The radio recombination lines detected at 1–2 mm wavelengths probe the ionized gas at distances of ~40 AU from the star (Martín-Pintado et al. 1989a), intermediate between the gas sampled at 15 GHz and at infrared wavelengths. The high intensity of the line emission at 1.3 mm makes it possible to study the dense ionized gas in the envelope at scales of some tens of astronomical units, possibly corresponding to the region where the disk is evaporating and forming an ionized outflow. In this paper we report interferometer observations of the H30α line (231.9 GHz) performed to measure the relative positions on the sky of the two velocity components in MWC 349.

2. OBSERVATIONS AND RESULTS

The observations of the H30α line ($\nu = 231.901$ GHz, $\lambda = 1.29$ mm) were made in 1991 February and March with the Owens Valley Millimeter Interferometer. The three 10.4 m antennas were equipped with SIS receivers with double-sideband receiver temperatures of 100–150 K. The antennas were positioned in two different configurations. On February 26 they were located 100 m north, 50 m west, and 50 m east of the track cross point. On March 7 the positions were 140 m north, 100 m west, and 100 m east. The synthesized beams were 1".5 × 1".3 (east-west by north-south) for the shorter baseline configuration, and 0".70 × 0".84 for the longer baseline configuration.

Spectral coverage was provided by a filter bank consisting of 32 × 5 MHz channels encompassing 207 km s^{-1} at a resolution of 6.5 km s^{-1}. Radio continuum measurements in both sidebands were simultaneously obtained using a 400 MHz continuum filter. The maser line was observed in the upper sideband of the receivers. MWC 349 was observed continuously for 10 hr in both configurations. The amplitude and phase of cross-correlated spectra obtained in the 100N–50W–50E configuration are shown in Figure 1. The weather was good during both observing runs, with a clear sky and inappre-

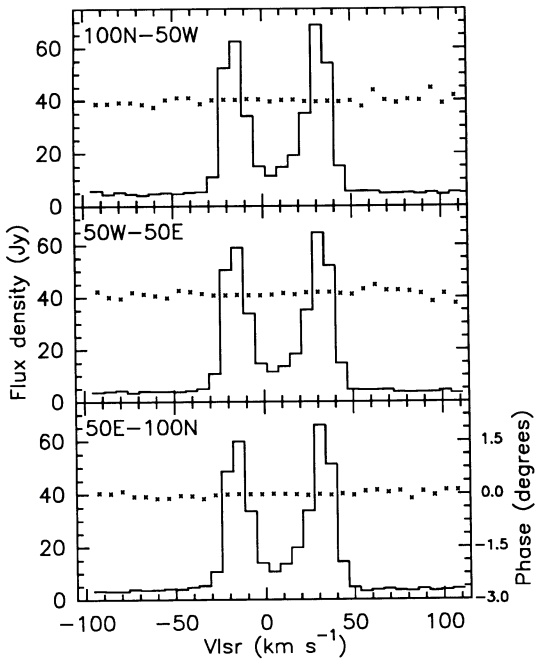

FIG. 1.—Spectra of the MWC 349 H30α recombination line ($\lambda = 1.29$ mm) obtained 1991 February 26 on the indicated baselines with the OVRO interferometer. These results are from a coherent integration of 3.5 hr during night time. The resolution was 5 MHz. The histograms indicate the amplitudes; the small crosses indicate the fringe phases.

ciable wind. The zenith sky opacity was 0.2 on February 26 and 0.5 on March 7, which resulted (in addition to the longer baselines) in lower coherence in the detected signals on March 7 (0.6 on March 7 versus 1.0 on February 26, measured toward 3C 273). A 3 hr observation of 3C 273 (for instrumental calibration; see below) and the first half of the observation of MWC 349 were done during the night and early morning. There was some loss of coherence (from 1 down to 0.6) a few hours after sunrise (i.e., for a positive hour angle for MWC 349), possibly due to changes in the atmosphere and in the pointing of the telescopes. In the data reduction (other than Fig. 1), the MWC 349 data points were weighted proportionally to the coherence and inversely to the system temperature of the corresponding baseline.

The absolute flux density scale was established from observations of Uranus ($T_B = 94$ K, diameter = 3.″5) and Neptune ($T_B = 92$ K, diameter = 2.″2), with appropriate corrections made for the expected visibilities of the planets and the primary beam of the antennas (34″). The correction for the visibilities was especially difficult due to the large diameter of the planets. Observations at different hour angles were necessary to have at least one measurement for each baseline in which the planet was not heavily resolved. This problem was particularly important for the longer configuration, because of the loss of coherence due to atmospheric effects and the longer baselines. In this case, we had to use 3C 273 as the main flux calibrator, for which we assumed a flux density of 30 Jy, obtained from the shorter baseline measurements. The continuum flux of MWC 349 was measured using the lower sideband continuum channel, which is not contaminated by the radio recombination line. The measured value of 1.67 ± 0.34 Jy is consistent with the single-dish measurement by Martín-Pintado et al. (1989a).

Our goal for the present observations was to determine the difference in the position of the two masers. We followed the method first described by Wright & Plambeck (1983), which consists in measuring the variation in time (i.e., in hour angle) of the phase difference between two given channels. For that purpose, a very good characterization of the passband response and of its time variations is required. Passband calibration was based upon 3 hr integrations on 3C 273. We did not find any evidence of significant variations in the individual 5 MHz channel phases, when referred to the continuum channel phase, over this period of time. The dispersion of the residual phases of the 5 MHz contiguous channels was less than 2° for each baseline for the shorter configuration, and less than 10° for the longer configuration. This result shows that the uncertainty in the measurement of relative positions, based on phase differences between channels, will be smaller for the data taken with the shorter baselines. However, phase ripples within the passband with a period of a few channels are not removed by the outlined procedure. To estimate their possible existence, we used the 3C 273 data to determine the variation in time of the difference between the average phase for three contiguous channels and the average phase for another set of three contiguous channels, corresponding to the frequency of the two maser components. The fact that the intensity of the continuum for 3C 273 was similar to (although smaller than) the intensity of maser lines for MWC 349 made it possible for us to check for such instrumental phase effects with the precision we needed to measure relative positions down to 0.″05 or smaller. We found no significant difference between the two phases that would lead to such an "instrumental" offset position larger than 0.″01, which can be considered as an upper limit for what would be reached on MWC 349 allowing for its higher intensity and longer integration time, i.e., better signal-to-noise ratio.

The first reduction of the MWC 349 data consisted in computing the phase difference between the average of three 5 MHz channels corresponding to the 32 km s^{-1} maser feature and three channels for the lower velocity feature (see Fig. 1), and fitting the phase differences $\Delta\phi$ to the expression

$$\Delta\phi = -2\pi(u_\lambda \Delta\alpha \cos\delta + v_\lambda \Delta\delta)$$

(Wright & Plambeck 1983), where u_λ and v_λ are the components of the projection of the baseline vector in the plane of the sky in units of wavelength, and $\Delta\alpha$ and $\Delta\delta$ are the relative coordinate offsets of the two spots that produce the maser features. Figure 2 shows the fits, and the numerical results are given in Table 1, together with the average values obtained for each baseline configuration. The uncertainties quoted in Table 1 refer to the rms deviation in the corresponding least-squares weighted fit, except in the case of the "average" of the three individual baseline results. In this case, the uncertainty reflects the scatter in the values derived for the three baselines. The agreement between the three baseline results may also indicate the absence of any passband drift on time scales larger than 3 hr. Notice that the uncertainties are a factor of 4 larger for the data taken on March 7, as a result of the poorer quality of the data (see above). The results for both dates, however, agree within the uncertainties. The (weighted) average value for the distance between the two spots is 0.″065 ± 0.″005, which corresponds to a projected separation of 80 AU, and the position angle is 107° ± 7°.

We have also generated six individual channel maps using AIPS in order to check the previous results. The peak position

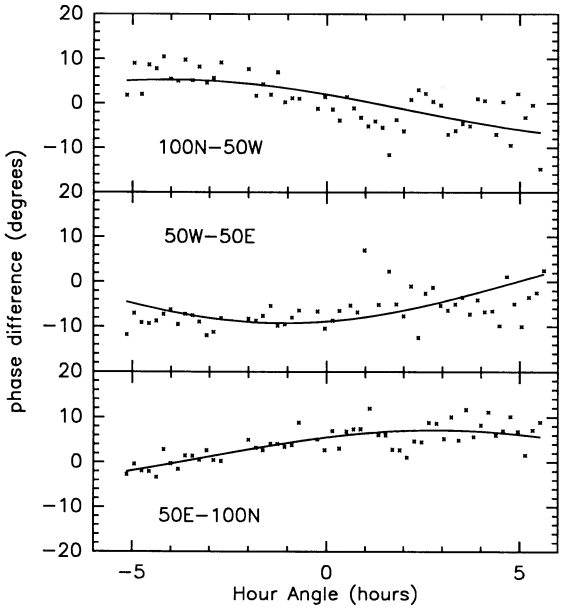

FIG. 2.—Results of the relative position determination for the 100N–50W–50E configuration. Each data point represents the phase of the 32 km s^{-1} maser component relative to that of the -16 km s^{-1} component. The integration time per point is 10 minutes. The smooth curves show the phase expected for the relative position determined for each baseline.

uncertainty in each channel due to noise is estimated to be smaller than $\pm 0''.008$. We did not find any significant trend in the peak position for the three contiguous channel sets centered in each line. The difference between the average position of the two peaks (see Table 1) is consistent with the previously quoted results. However, we prefer the first method for determining the relative positions because the data fitted individually for each baseline have suffered less manipulation, and the method gives three independent values.

3. DISCUSSION AND CONCLUSIONS

An early attempt to explain the presence of the two maser features was the suggestion by Martín-Pintado et al. (1989b) that emission originates in the opposite lobes of the ionized bipolar outflow. Model calculations showed that values for density, opacity, and stimulated emission ($\beta_n < -1$) were consistent with maser emission taking place. Furthermore, the observed time variability of the two components of the maser emission (Martín-Pintado et al. 1989b; Thum, Martín-Pintado, & Bachiller 1992) can be accounted for by time changes in the rate of mass accretion into the central star and, therefore, in the ionized bipolar outflow that results from accretion. One may then think of both velocity components originating in the bipolar outflow, as first suggested by Martín-Pintado et al. (1989a), and of the outflow as being slightly asymmetric. A different radial distribution of ionized gas in the jets is required to explain the different intensity and different time variations of the two components, and would also explain the observed propagation of such variations to larger distances from the star (Martín-Pintado et al. 1989b). Another asymmetry is required if the (unknown) stellar velocity is assumed to be 1 km s^{-1}, as measured from nonmaser lines (e.g., H41α; cf. Thum et al. 1992), which differs by 7 km s^{-1} from the average velocity of the maser peaks. In this situation, the misalignment between the axis of the two ionized jets is $\sim 20°$.

Another attempt to explain the shape and variability of the radio recombination maser lines was made by Ponomarev et al. (1989) in the frame of a disk plus bipolar jet model. In such a model, the blue emission (-16 km s^{-1}) is assumed to arise in the ionized jet oriented toward us inclined $\sim 10°$ to the plane of the sky, and the 32 km s^{-1} emission is suggested to originate in the gas falling toward the star in the near part of an accretion disk which is being ionized by the stellar radiation. However, the presence of ionized gas falling at ~ 40 km s^{-1} toward the star is not easily explained, and such a gaseous component has not been found at other wavelengths.

On the other hand, over the last few years evidence for the existence of an edge-on dusty circumstellar disk around MWC 349 has increased. The first suggestion came from Cohen et al. (1985), who explained the geometry of the 5 GHz radio continuum map, the low infrared luminosity, and the extinction excess, as caused by the presence of such a disk. The neutral disk seems to be edge-on and lying approximately in the east-west direction (P.A. $\sim 100°$). The structure of the radio continuum emission also shows the presence of a less than $0''.1$ wide dark lane separating two lobes of ionized gas (White & Becker 1985). Leinert (1986) has measured the east-west size of the circumstellar dust distribution by 3.8 μm speckle interferometry. Assuming a Gaussian shape for the brightness distribution, the measured full width at half-maximum is $0''.086 \pm 0''.019$. The north-south distribution was marginally re-

TABLE 1

POSITION OF THE BLUESHIFTED RELATIVE TO THE REDSHIFTED COMPONENT

Baseline	cos $\delta\,\Delta\alpha$	$\Delta\delta$	Distance	P.A.	Comments
		1991 February 26			
100N–50W	$-0''.0631 \pm 0''.0007$	$0''.0165 \pm 0''.0005$	...	...	Weighted data fit
50W–50E.....	-0.0693 ± 0.0005	0.0260 ± 0.0007	...	...	Weighted data fit
50E–100N	-0.0595 ± 0.0005	0.0121 ± 0.0003	...	...	Weighted data fit
Average	-0.0640 ± 0.0050	0.0182 ± 0.0071	$0''.066 \pm 0''.005$	$106° \pm 6°$	Nonweighted average
Maps	-0.063 ± 0.010	0.012 ± 0.013	0.064 ± 0.010	101 ± 12	AIPS image fit
		1991 March 7			
140N–100W.....	$-0''.0697 \pm 0''.0032$	$0''.0408 \pm 0''.0024$	...	...	Weighted data fit
100W–100E	-0.0365 ± 0.0013	0.0156 ± 0.0023	...	...	Weighted data fit
100E–140N	-0.0323 ± 0.0025	0.0136 ± 0.0018	...	...	Weighted data fit
Average	-0.0462 ± 0.0205	0.0233 ± 0.0152	$0''.052 \pm 0''.020$	$117° \pm 18°$	Nonweighted average
Maps	-0.054 ± 0.009	0.006 ± 0.011	0.054 ± 0.009	96 ± 12	AIPS image fit

solved (0".038 ± 0".018), which Leinert took as further evidence for the edge-on, disk-shaped distribution of the circumstellar dust. The most detailed knowledge of the kinematics of the ionized gas around MWC 349 comes from the infrared spectroscopy carried out by Hamann & Simon (1986, 1988). Although there are some difficulties in locating the gas responsible for each of the observed lines, these line profiles can be explained by assuming a dense rotating neutral disk, a bipolar ionized wind, and a partially ionized interface region. The rotation of the disk is required to explain the large number of double-peaked lines (some of them are forbidden lines), which cannot be produced by self-absorption. In their model, the ionized wind does not originate in the star itself but is produced by photoionization of the neutral disk dense regions closest to the star (located at a few AU from it). The densest ionized gas will be found close to the neutral disk, making the most likely location for the maser line emitting regions the ionized surface of the neutral disk.

The previous discussion has led us to two configurations for the maser emission, two ionized jets, or ionized gas near the neutral rotating disk. The relative position of the two sources turns out to be the key to discriminating between those options, since the sources would appear in the first case in approximately the east-west direction and in the latter case in the north-south direction. Our measurement of the relative position shows that the 32 km s^{-1} component originates in a region located approximately east of the -16 km s^{-1} emitting region with a position angle of 107°, very similar to what is found for the dark lane in radio continuum observations (White & Becker 1985). Therefore, the results of our observations suggest that *the maser emitting regions are closely associated with the disk.*

Simple modeling of the radio continuum spectrum by Martín-Pintado et al. (1989a) allows the determination of the distance to the star at which the ionized wind continuum emission becomes optically thin at 230 GHz, and consequently at which the H30α line can be detected. Such a distance is of the order of the projected distance between the red and blue maser spikes. Due to radio continuum opacity effects, one would expect to detect the maser recombination lines blueshifted with respect to the systemic velocity of the stellar wind detected at lower frequencies, for a purely expanding wind. However, what is observed is exactly the opposite. For ionized gas dragged by a purely rotating disk, the line emission can be explained as produced in two spots located east and west of the star. The dense ionized gas responsible for the maser lines is likely to be rotating, dragged by the neutral disk, and also expanding, due to stellar wind and pressure effects.

In any of these situations the main question to be answered concerns the presence of maser emission localized in only two spots. The high-density ionized gas localized in a few large clumps is an obvious possible explanation. Since the maser emission is strongly dependent on the line optical depth, currently only two clumps in the near side of the disk are detected.

These are further arguments in favor of a rotating, clumpy disk. The decrease in the velocity separation of the two peaks found in atomic lines observed at near-IR wavelengths (Hamann & Simon 1988) is correlated with the excitation of the lines. The farther away from the star the lines originate, the smaller the peak-to-peak distance is. For some neutral gas tracers which require lower energy photons to be ionized (e.g., [Fe II], [Cr II]), distances between the two peaks of 40–50 km s^{-1} have been measured, similar to what is found in radio recombination maser lines. This argument was used by Hamann & Simon (1986) to conclude that the circumstellar disk is rotating.

Since the *two maser components originate in two different places in the disk*, their independent time behavior is easily explained, intensity time variations being caused by irregularities or changes in the disk mass distribution. There already are some hints of the existence of irregularities in the neutral gas distribution, obtained from optical polarization measurements. Optical emission is highly (8%–10%) polarized (Elvius 1974; Zickgraf & Schulte-Ladbeck 1989), the position angle (160°–170°) being roughly (but not exactly) perpendicular to the disk, which suggests that the bulk of the polarization is produced through scattering in the dusty disk. The detected daily variations in the degree of polarization while its position angle remains constant (Bergner et al. 1987) indicate that the polarization variability is caused by changes in physical conditions (density, column density) of the neutral gas rather than changes in the overall scattering-medium geometry. Long-term monitoring of the maser variability (Thum et al. 1992) has shown antisymmetrical changes of a few kilometers per second in the radial velocities of the blue and red components, which are explained by small changes of the stellar luminosity.

In conclusion, our observations support the existence of a nearly edge-on neutral disk around MWC 349, which is the source of the high-density ionized gas responsible for the millimeter-wavelength recombination lines. The observational facts that the two maser components originate in two spots (this paper) and that the centroid velocity is redshifted with respect to the systemic velocity (Martín-Pintado et al. 1989a), can be explained by the presence of a few higher density clumps (two of them detected) of ionized gas located in the near part of the rotating disk.

We thank the Owens Valley Radio Observatory staff for their assistance during the observations. P. P. thanks N. Scoville and J. D. Kenney for their hospitality during his stay at Caltech for the data reduction. The Owens Valley Millimeter Interferometer is supported by NSF grant AST 90-16404. This work has been partially supported by the Spanish CICYT under grants PB 88-0408 and URC 23/91.

REFERENCES

Bergner, Y. K., et al. 1987, Soviet Astron. Lett., 13, 84
Cohen, M., Bieging, J. H., Dreher, J. W., & Welch, W. J. 1985, ApJ, 292, 249
Elvius, A. 1974, A&A, 34, 371
Hamann, F., & Simon M. 1986, ApJ, 311, 909
———. 1988, ApJ, 327, 876
Harvey, P. M., Thronson, H., & Gatley, I. 1979, ApJ, 231, 115
Leinert, C. 1986, A&A, 155, L6
Martín-Pintado, J., Bachiller, R., Thum, C., & Walmsley, M. 1989a, A&A, 215, L13
Martín-Pintado, J., Thum, C., & Bachiller, R. 1989b, A&A, 222, L9
Olnon, F. M. 1975, A&A, 39, 217
Ponomarev, V. O., Smirnov, G. T., Strelnitskij, V. S., & Chugai, N. N. 1989, Astron. Tsirk., 1540, 5
Thompson, R. I., Strittmatter, P. A., Erickson, E. F., Witteborn, F. C., & Strecker, D. W. 1977, ApJ, 218, 170
Thum, C., Martín-Pintado, J., & Bachiller, R. 1992, in preparation
White, R. L., & Becker, R. H. 1985, ApJ, 297, 677
Wright, M. C. H., & Plambeck, R. L. 1983, ApJ, 267, L115
Zickgraf, F.-J., & Schulte-Ladbeck, R. E. 1989, A&A 214, 274